Vladimir Savcenko, MD
Bradley J. Erickson, MD, PhD
Patrice M. Palisson, PhD
Kenneth R. Persons, MS
Armando Manduca, PhD
Thomas E. Hartman, MD
Gordon F. Harms, MD
Larry R. Brown, MD

Author contributions:
Guarantors of integrity of entire study, V.S., B.J.E.; study concepts, B.J.E.; definition of intellectual content, B.J.E.; literature research, V.S., A.M.; experimental studies, V.S., K.R.P., T.E.H., G.F.H., L.R.B.; statistical analysis, V.S., B.J.E., P.M.P., A.M.; manuscript preparation, V.S., B.J.E., K.R.P., A.M., P.M.P.; manuscript editing, P.M.P.

Detection of Subtle Abnormalities on Chest Radiographs after Irreversible Compression[1]

PURPOSE: To assess the effect of wavelet-based compression of posteroanterior chest radiographs on detection of small uncalcified pulmonary nodules and fibrosis.

MATERIALS AND METHODS: Computed tomography (CT) of the chest was used to identify 20 patients with normal posteroanterior chest radiographs, 20 with a solitary uncalcified pulmonary nodule 1–2 cm in diameter, and 20 with fibrotic disease. A double-blind protocol for readings of original images and images compressed at 40:1 and 80:1 was analyzed by using the nonparametric receiver operating characteristic to measure differences in diagnostic accuracy and their statistical significance.

RESULTS: There was no substantial difference in the overall diagnostic accuracy (measured by the area under the curve index) for both nodules and fibrosis between images compressed at 40:1 and 80:1 and uncompressed images. Readers tended to perform better on images compressed at 40:1 compared with uncompressed images. The "high-sensitivity" portion of the 80:1 compression curve for nodules was below that for the uncompressed curve, although this was not statistically significant.

CONCLUSION: Lossy compression of chest radiographs at 40:1 can be used without decreased diagnostic accuracy for detection of pulmonary nodules and fibrosis. There is no statistically significant difference in diagnostic accuracy at 80:1 compression, but detection ability is decreased.

The development of digital imaging technologies over the past 20 years has made the idea of filmless radiology feasible. Filmless radiology is essential for the implementation of hospital picture archiving and communication systems and teleradiology applications at many locations around the world. It is hoped that digital images will be more efficiently and easily managed and retrieved at any computer workstation within the hospital, which would increase overall efficiency. Teleradiology also makes it possible to send these digital radiologic images to other hospitals or homes for rapid consultation or review.

However, several social, economic, and technical barriers still prevent complete acceptance and restrict the wide deployment of digital imaging in radiology departments (1). Among technical and practical limitations is the large size of high-resolution images (typically several megabytes), which necessitates long communication times across network or telephone lines. Image production within a large all-digital radiology department could produce several terabytes (10^{12} bytes) of information per year (2). The cost of storing these images in a fashion that would make them accessible in a reasonable time would be substantial.

The solution to the image size problem is compression. Lossless compression methods use redundancy within an image to reduce the size of the image file yet allow perfect reconstruction. These lossless techniques have the obvious appeal of perfect image reproduction, but they achieve only 2:1 to 3:1 reduction for medical images (3). On the other hand, lossy techniques can reduce images by any desired ratio, with higher ratios

resulting in a less faithful reproduction of the original. Ratios up to 100:1 may be acceptable in some circumstances (4).

Several studies have been performed to investigate the effects of compression on image distortion and diagnostic degradation (3,5–8). Because of the difficulty and cost of rigorous design and evaluation, most studies have been limited to quantitative measurements or image assessments by less experienced observers. The purpose of this study was to evaluate the effect of wavelet-based compression of chest radiographs on detection of subtle findings.

MATERIALS AND METHODS

Case Selection

Two types of abnormality were chosen for this study: solitary pulmonary nodules (selected as a model of a low-contrast, low-frequency—ie, with a slowly changing shape—abnormality) and fibrosis (selected as a model of a higher frequency—ie, with sharp edges—abnormality). The origin of the finding was not considered; the appearance of pathologic findings was the only criterion. An effort was made to select particularly subtle cases. Each nodule had to be solitary, uncalcified, and 1–2 cm in diameter. Each instance of fibrosis had to be described on the original radiograph evaluation as a mild or borderline case or as "possible" fibrotic changes with the recommendation for further diagnostic investigation.

This protocol was reviewed and approved by our Institutional Review Board. Thoracic computed tomographic (CT) examinations were performed within 30 days of the posteroanterior (PA) chest radiography, and the CT results were used retrospectively to identify 20 patients each with findings in one of three categories: (a) normal (no abnormality of any type); (b) a solitary uncalcified pulmonary nodule 1–2 cm in diameter, always confirmed with biopsy; and (c) fibrotic disease. Thus, a total of 60 cases were used for this study.

Image Compression

The conditions of original image acquisition were as follows: screen-film system (InSight; Eastman Kodak, Rochester, NY), screen-film system speed of 250, 120-inch source-image distance, 120 kVp, 600 mA, time determined by automatic exposure control (for an average male patient, PA image requires 15 mAs), and scatter-reduction device focused 12:1 with 152 line per inch grid.

Each PA chest radiograph was digitized

at approximately 2,000 × 2,500 pixels with 12 bits per pixel by using a system based on a laser scanner (Lumisys 200; Eastman Kodak). The resulting 60 files were compressed at 40:1 and 80:1 and then decompressed by using a wavelet-based algorithm. This algorithm computes a discrete wavelet transform for each image, followed by a coding of the wavelet coefficients with an algorithm called set partitioning in hierarchical trees (SPIHT), which was proposed by Said and Pearlman (9) and adapted for medical images by Manduca (10). The discrete wavelet transform uses the 9-tap/7-tap biorthogonal filters of Antonini et al (11) to obtain a five-level decomposition of the original image. The SPIHT algorithm provides excellent image quality at a given compression ratio, fully progressive transmission, and the ability to compress an image exactly to any specific number of bytes.

After compression and decompression, 180 digital files existed: 60 original images, 60 images compressed and decompressed at 40:1, and 60 images compressed and decompressed at 80:1. The images were reproduced at full size. A look-up table was applied to the 180 files to compensate for differences in calibration of the digitizer and printer. The matching of these laser-produced images with original images was validated visually and through optical densitometric measurements. The images were printed with a laser printer (Ektascan; Eastman Kodak).

Reading Protocol

Three board-certified radiologists with subspecialty training in thoracic imaging were used as evaluators. A double-blind protocol was employed, in which neither the radiologist nor the experimenter was aware whether a particular image was uncompressed or compressed at 40:1 or 80:1. Images were viewed on a standard clinical illuminator in a darkened room, and all were placed on the illuminator at the same time except the last 20 images because the capacity of a standard illuminator is 160 images. During a short break, the first 20 images (which had already been read by particular radiologist) were replaced with the final 20 images. The order of image presentation was determined by means of a pseudorandom number generator, which created a mixture of uncompressed and compressed images.

Radiologists were asked to provide an evaluation separately for presence of fibrosis and for presence of nodule, each on a scale of 1–5, where 1 = definitely not

present, 2 = most likely not present, 3 = possibly present, 4 = most likely present, and 5 = definitely present. The radiologists were encouraged to use the full range of ranking levels. In the case of a positive finding of a nodule (any category but "1"), they specified the position of the nodule on a sketch of the lungs. The diagnosis was considered correct if horizontal and vertical deviation from the CT-proved location of the nodule was no more than 15% of the width or height of the lungs, respectively.

Evaluation of Radiologists' Ratings

The performance of the diagnostic system, composed of the film-viewing display and the three radiologists, was evaluated with a standard receiver operating characteristic (ROC) method, which is widely used in radiology (5,12–15). ROC curves were constructed for the readings of original images and images compressed at 40:1 and at 80:1 for each radiologist and also for the combined radiologists' readings. A z-score test was used to determine whether the difference of the area under the curve (AUC) indexes of two given ROC curves was statistically significant.

No assumption was made about a possible Gaussian distribution of the confidence ratings, and only nonparametric tests were performed. Thus, the AUC indexes were directly obtained by means of trapezoidal approximation of the surface beneath the curves, and their variances were estimated from the case-sample variance, between-reader variance, and within-reader variances (16). A different assumption, easier to meet with sufficiently large case samples, is that the AUC indexes are normally distributed, so that $(AUC_1 - AUC_2)/SD(AUC_1 - AUC_2)$—where SD is the standard deviation—follows a z statistic, which we believe applies to the current study on the basis of criteria specified by Swets and Pickett (16).

Numerical Evaluations

In addition to the evaluation of diagnosis degradation, a set of quantitative distortion measurements between original and compressed images was computed: signal-to-noise ratio, average pixel error, maximum pixel error, and root mean square error.

RESULTS

Tables 1 and 2 summarize the radiologists' ratings for fibrosis and nodule, re-

TABLE 1
Readings for Fibrosis by All Three Radiologists

| | Confidence Rank | | | | |
	1	2	3	4	5
Diagnosis					
Uncompressed					
True-negative	52	28	23	11	6
True-positive	4	13	7	16	20
Compressed at 40:1					
True-negative	57	35	6	18	4
True-positive	6	9	8	14	23
Compressed at 80:1					
True-negative	52	29	15	18	6
True-positive	2	17	6	12	23

Note.—True-negative groups the 120 readings of the 40 images that are not fibrosis, that is, normal and nodule images. True-positive represents the 60 readings of the 20 fibrosis images.

TABLE 2
Readings for Nodules by All Three Radiologists

| | Confidence Rank | | | | |
	1	2	3	4	5
Diagnosis					
Uncompressed					
True-negative	64	36	16	4	0
True-positive	12	4	0	11	33
Compressed at 40:1					
True-negative	68	33	16	3	0
True-positive	10	5	1	13	31
Compressed at 80:1					
True-negative	62	37	15	6	0
True-positive	9	5	4	12	30

Note.—True-negative groups the 120 readings of the 40 images that are not nodules, that is, normal and fibrosis images. True-positive represents the 60 readings of the 20 nodule images.

spectively. In each table, all readings on images that did not have the considered abnormality were labeled as negative. For instance, for the data in Table 1 (fibrosis), both normal and nodule images were considered "negative." In the nodule analysis, no negative image was ranked to be certain abnormality (rank, 5), but a substantial number of images with nodules were missed (rank, 1) on both uncompressed and compressed images. We believe this reflects the subtlety of the findings in the cases selected for this study.

Figure 1 shows the absolute pixel differ-

ence images for a case of fibrosis and a case with a nodule at 40:1 and 80:1 compression ratios. A narrow width (1% of original display window setting) was used to emphasize the distribution of errors across the image. Errors are almost uniformly distributed in the space, although each image shows a clear correlation with anatomic structures at 80:1. Figure 2 shows a subtle nodule and a lung area containing fibrosis, displayed with narrower width to provide contrast enhancement. Both nodules and fibrosis are well preserved even at 80:1 compression. In fibrosis cases, where subtle signs on images cannot be as precisely localized as nodules, a global examination of magnified images did not exhibit a noticeable difference at either 40:1 or 80:1. Radiologists commented verbally on the difficulty of identifying which images might be compressed, and none commented on objectionable artifacts.

ROC Analysis

Figure 3 shows the averaged ROC curves for all three radiologists for fibrosis and nodule. Figure 4 shows the ROC curves for each radiologist separately for nodule and for fibrosis plotted assuming a Gaussian distribution. (In each abnormality consideration, both actual negative cases and cases with different abnormalities were considered negative. Thus, for example, nodules were compared to "negative" cases, which comprise actual negative cases and fibrosis cases.) Table 3 shows the probabilities that any difference in AUC indexes from two different ROC curves was significant. AUC indexes were always higher with compressed images than original images for both nodules and fibrosis. There was virtually no difference between compression at 40:1 and compression at 80:1, with confidence levels of 0.82 and 0.91, respectively.

Quantitative Measures of Distortion

We measured the distortion parameters on regions of interest centered around each nodule or within areas showing most prominent fibrosis. Neither local nor global measurements seemed to be correlated with diagnostic degradation. Other authors have also attempted to correlate observation with numerical measures, but no results have been satisfactory (17–20).
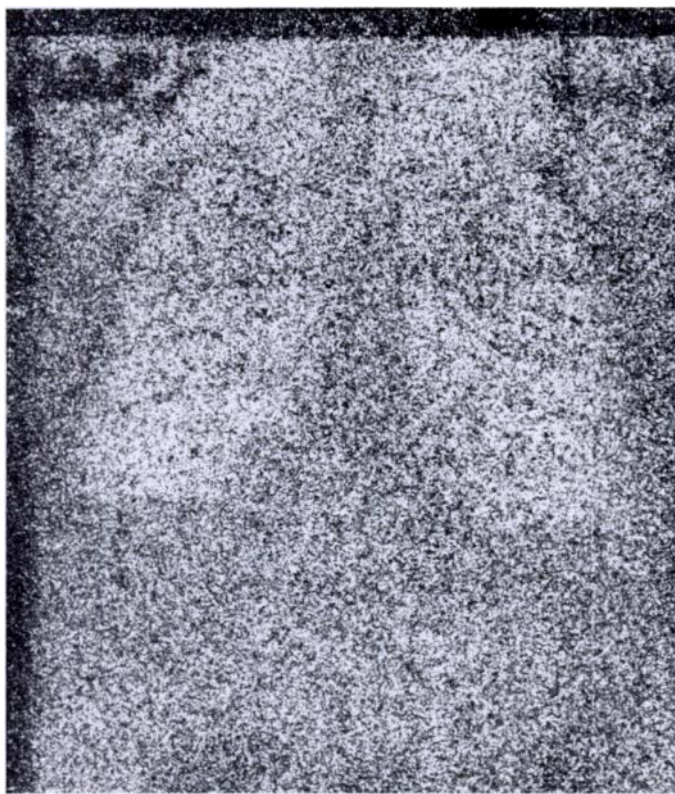
DISCUSSION

Evaluation of the effects of compression is an important and challenging task if

one considers that important benefits would accrue if medical images could be compressed within the acquisition device, before primary diagnosis. The cost of a picture archiving and communication system would be substantially reduced if lossy compression could be used throughout the entire system. The U.S. Food and Drug Administration allows medical device manufacturers to report the normalized mean square error as a measure of image degradation when lossy compression techniques are used (21), although this measure is of limited value. Therefore, studies of individual modalities and abnormalities, such as the present one, contribute to the Food and Drug Administration's approval of a given compression scheme and of its acceptance for routine use in clinical practice.

The ROC curves shown in Figures 3 and 4 indicate that, with our algorithm, compression up to 80:1 does not degrade the diagnosis of lung nodules or fibrosis, even in subtle cases. In fact, the variability of the results is greater between radiologists than between different compression ratios. Furthermore, the results suggest that compression at 40:1 may increase the accuracy of the diagnosis (possibly due to the reduction of noise [7]), although this was not a statistically significant difference. At 80:1 compression, the accuracy of diagnosis is always higher than that for uncompressed images, but by less than 1 standard deviation.

The maximum compression level for a given image not only is characteristic of the image but also varies as a function of several parameters including the abnormality to be detected, the type of display used for readings, and the level of expertise of viewers. Examination of all 20 nodules in this study showed that they were always well preserved even at 80:1 compression, as shown in Figure 2. A nodule is a low-frequency structure that is quite tolerant to compression by wavelet-based algorithms (8). Fibrotic disease tends to be of higher frequency and is less well preserved. Nevertheless, the 40:1 SPIHT wavelet compression appears to be acceptable for primary diagnosis of nodules and fibrosis based on chest radiograph evaluation.
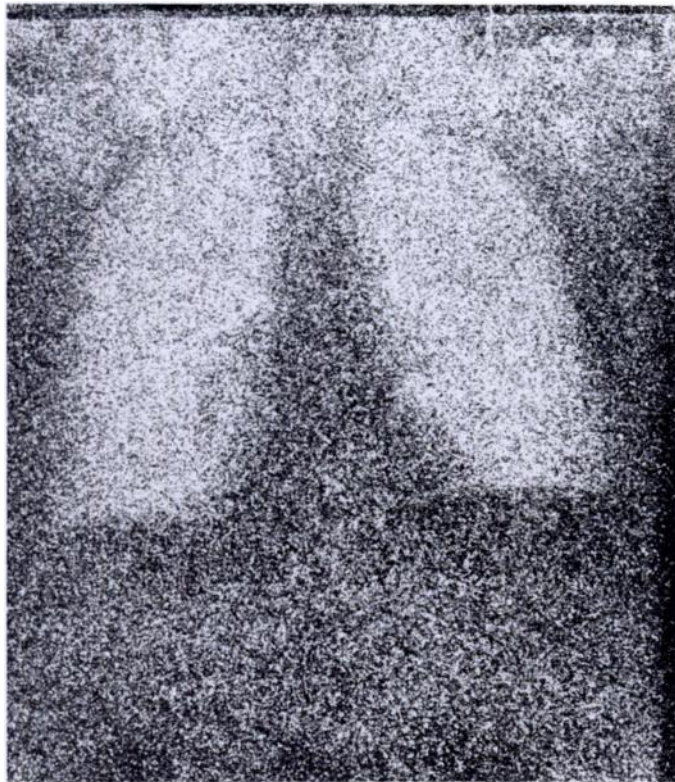
Similar studies performed to evaluate compression schemes based on discrete cosine transform have shown a substantially lower acceptable compression ratio. MacMahon et al (22) used a proprietary 16 × 16 discrete cosine transform–based compression technique and concluded that a compression ratio of 25:1 was acceptable for similar digitized chest ra-

a.
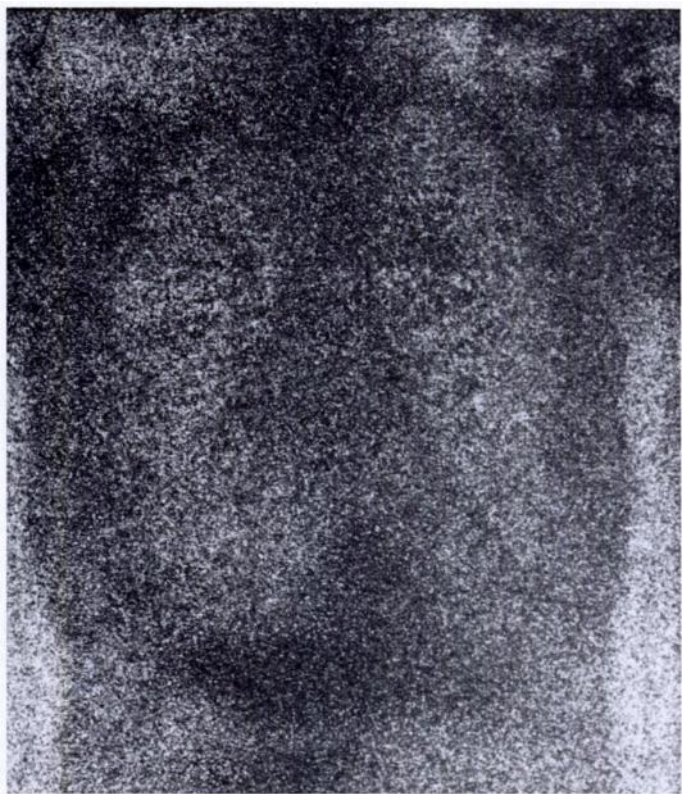
c.

b.

d.

Figure 1. Absolute pixel difference images at 40:1 and 80:1 compression ratios, for two typical digitized images representing a case with nodule and a case with fibrosis. (a) Nodule at 40:1 compression. (b) Nodule at 80:1 compression. (c) Fibrosis at 40:1 compression. (d) Fibrosis at 80:1 compression. Maximum pixel difference on all 120 compressed images was 111, for a typical pixel range of 0 to about 2,800. Difference images are shown with the same contrast enhancement, defined by a window of 20 and a level of 10. Errors between 0 and 20 are represented in a full black-and-white scale (any error above 20 is displayed as white). Figure 2 shows regions of interest (both original and after compression) for these images.
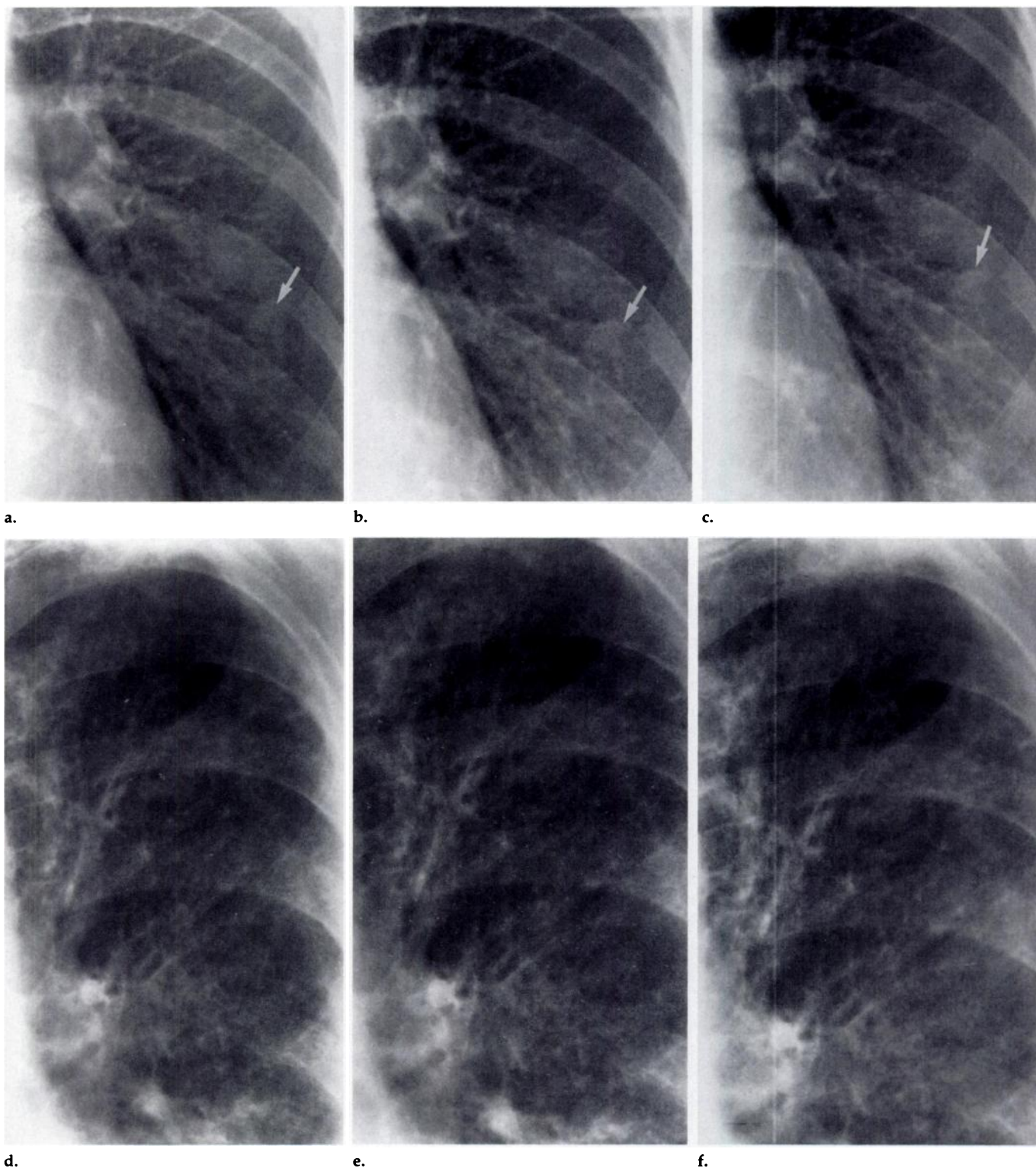
a.   **b.**   **c.**

d.   **e.**   **f.**

Figure 2. Region of interest in a case of a subtle nodule (arrow in **a–c**) and fibrosis. **(a)** Original image shows nodule. **(b)** Same ROI at 40:1 compression. **(c)** Same ROI at 80:1 compression. **(d)** Original image shows fibrosis. **(e)** Fibrosis at 40:1. **(f)** Fibrosis at 80:1. Figure 1 shows the absolute pixel errors over the entire images.

diographs of interstitial infiltrates and nodules. In another study, Sayre et al (23) used a full-frame discrete cosine transform technique and found no statistically

significant degradation of diagnosis at compression of 20:1 between original analog images, uncompressed images, and compressed digitized images of intersti-

tial disease at similar resolution. Using computed radiographic images, Ishigaki et al (24) found that plain computed radiographic chest images showed a statis-
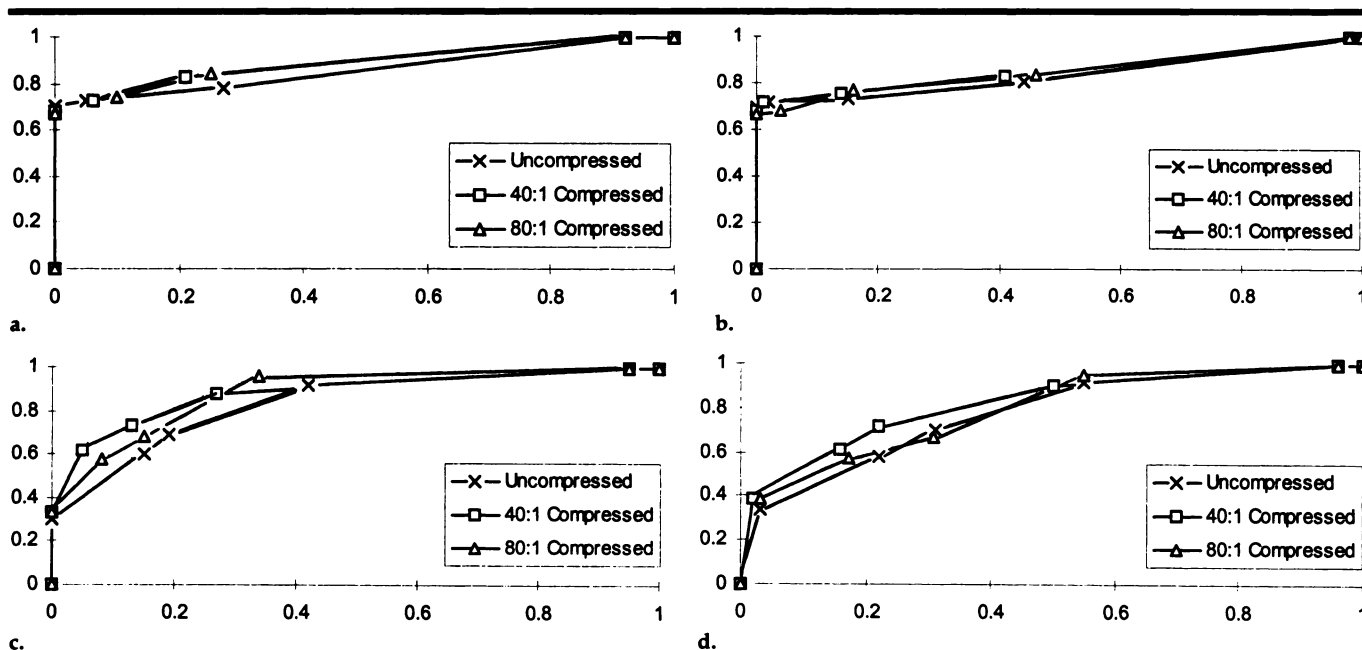
Figure 3. Averaged ROC curves for all three radiologists. (a) Nodule versus normal. (b) Nodule versus all others. (c) Fibrosis versus normal. (d) Fibrosis versus all others.

tically significant degradation at 25:1 compression, but the resolution of these images was lower and evaluation was performed on cathode-ray-tube monitors. In all three studies, although no statistically significant difference existed at these compression ratios, the trend was for compression images to be worse than the original. By contrast, in our study, compression images tended to be better.

Most radiologic modalities are expected to enable diagnosis of many different pathologic conditions. This raises questions about what is the most effective pathologic condition and image set for investigation of acceptable compression techniques. Goldberg et al (25) analyzed data from six images including radiographs of the chest, bone, and abdomen. Because of unique image characteristics of each anatomic structure, this approach might be valid for comparison of compression effects, but the assessment of diagnostic accuracy is doubtful. Cox (6) placed artificial pulmonary nodules into chest radiographic images. The ability to manipulate location, diameter, subtlety, and number of "nodules" is convenient, but the "unnaturalness" of the abnormality limits generalization of the results to clinical practice.

We have investigated two important pathologic conditions found on chest radiographs. The approximately 20% miss rate for nodules seen in this study likely reflects our selection of subtle cases. This

miss rate is in keeping with previously published reports on nodule detection on chest radiographs (26). One can expect that the diagnostic error encountered in routine cases on the same kind of compressed images should be lower; thus, our study should give a worst case estimate of the degradation due to lossy compression. We used CT, and biopsy in the case of nodules, which is a very high quality and unbiased "gold standard." Many studies use results on original images as the standard, which is biased against compression because any difference would be interpreted to mean the compressed image has been degraded (27).

Methodologic Criticisms

After the readings were performed, it was found that although the order of presentation was determined by a pseudo-random number generator, more uncompressed versions of images had been presented in the first set, that is, before the compressed versions were shown. Because the study was performed with a double-blind protocol, this was not detected until after the readings were performed. To detect a possible learning effect, we considered the difference in diagnostic accuracy between two complementary sets of cases. The first consisted of cases presented first as uncompressed and subsequently shown as compressed versions (both 40:1 and 80:1), whereas

the latter comprised cases shown in the opposite order (ie, compressed images presented first). This analysis was negative; it showed better performance for compressed versions presented either before or after uncompressed ones. Furthermore, the difference favoring compressed images was slightly bigger when compressed versions of images were presented first. On that account, if there was any gain due to learning effect, it favored (with no statically significant difference) reading of the uncompressed versions.

The statistical tests were based on the null hypothesis—the AUC is the same for the two ROC curves considered—which is different from the hypothesis that the curves are identical. For certain applications in which the socioeconomic cost of a "miss" is substantially higher than the cost of a false-positive result, other parameters could be used, such as a measure of differences between the ROC curves in the high sensitivity area (15). While some have questioned the value of the ROC study because of unrealistic assumptions and tasks considered unnatural (28), this method remains the most credible and acceptable method for diagnostic evaluation (13).

Another important consideration is the number of cases and observers used. One might argue that the negative result (no difference between compressed data) is due to too few observations. Eventually, when enough cases have been acquired,
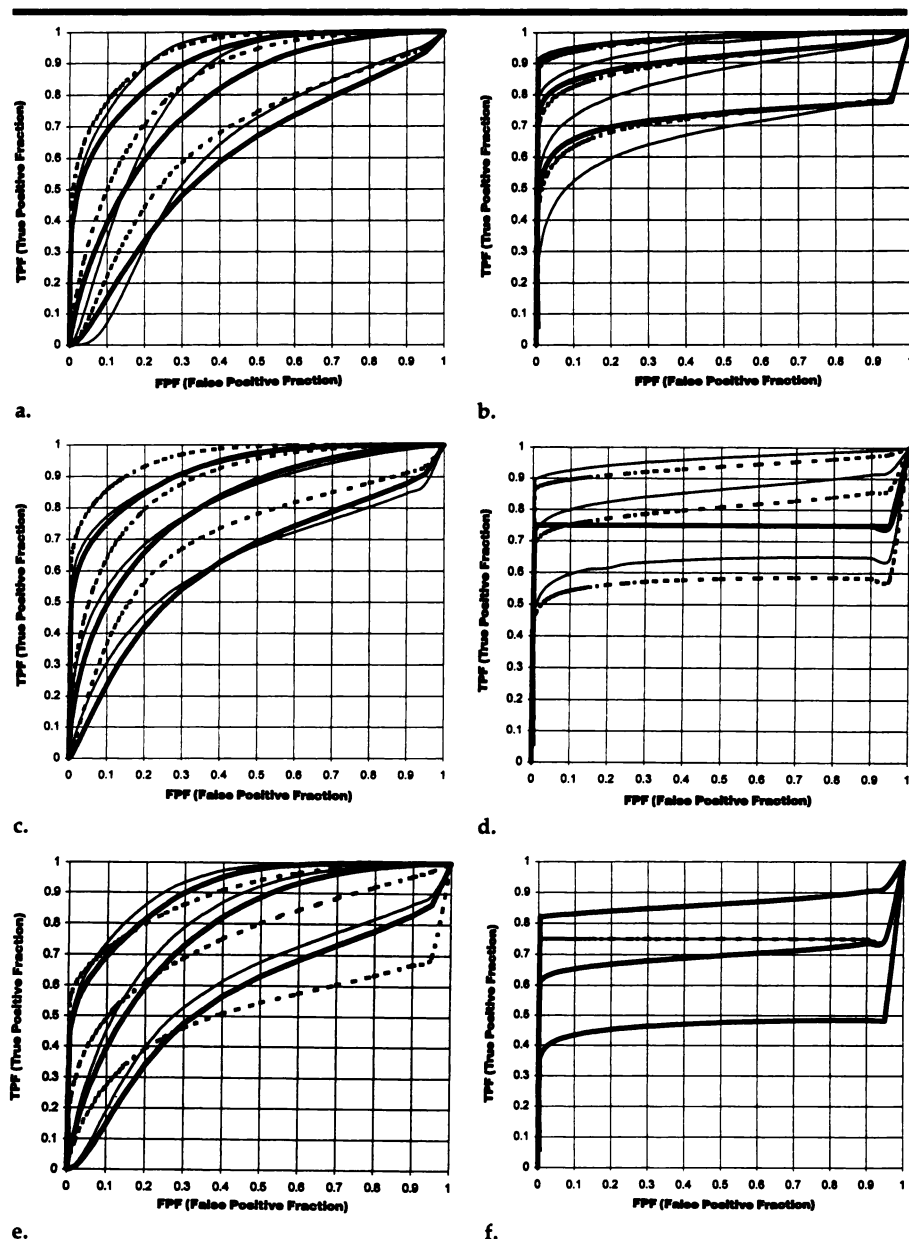
Figure 4. ROC curves plotted for individual readers, assuming a Gaussian distribution of the ratings, along with their 95% confidence intervals. For each chart, the solid thick line represents the curve for uncompressed images, the dotted line represents the curve for 40:1 compressed images, and the solid thin line represents the curve for 80:1 compressed images (the same style is used for upper and lower bounds of the intervals). (a) Reader 1 and fibrosis. (b) Reader 1 and nodule. (c) Reader 2 and fibrosis. (d) Reader 2 and nodule. (e) Reader 3 and fibrosis. (f) Reader 3 and nodule.

some sort of difference might be detected, but the trend suggests that it would show an advantage for compressed images.

Earlier theoretical work on ROC analysis (12) has shown that when one test set is derived from another (ie, compressed is derived from uncompressed, as opposed to, say, CT vs radiography), substantial increases in statistical power are realized. The z test becomes more sensitive to differences as the correlation R between

the two compared ROC curves becomes higher. Thus, compared to a test in which ROC curves are obtained from two independent data sets of size N, the statistical power is virtually the same as if the number of cases were $N' = N/(1 - R)$.

In our case, the average correlation coefficient between ratings on compressed and uncompressed images was approximately 0.80, and AUC indexes were between 0.77 and 0.88. Using the values in

the table in reference 12, we obtain the same sensitivity as if we had approximately 240 cases from independent data sets.

For nodules, the shape of the high-sensitivity area (false-positive fraction is near 1) of the ROC curves is due to the natural character of this pathologic condition, which tends to shift quantitative ratings of each case into binary decisions (eg, yes or no) as opposed to the more gradual rating of fibrosis cases (more extensive disease increases certainty). Another explanation for the shape of the curves was that the set of images was intentionally composed of very subtle cases, supported by a total of 20% of actual nodule cases being classified as "definitely not present."

Qualitative versus Quantitative Measurements

It would be very desirable to establish a correlation between subjective readings and objective computable parameters to characterize the difference between the original image and its compressed version; thus, only quantitative measurements would be required to assess the image quality. To our knowledge, however, no such measures are available.

Noise Removal

The wavelet transform itself is a lossless step. In wavelet compression, information is lost during the quantization step, as the exact values of the coefficients are replaced by approximate values. At low compression ratios, the effect of this approximation is to suppress noise. Indeed, this approximation is very similar to those of standard statistical wavelet denoising algorithms (29). The result of such noise removal is to make the image more appealing to the observer's eye without degrading diagnostically relevant details such as tissue texture or anatomic structure information. Thus, lossy compression does not necessarily imply a decrease in the radiologist's performance. There is evidence that radiologists prefer slightly compressed images (eg, 2,048 × 2,560 × 12 digitized chest radiographs compressed at 10:1) over original images (6,7). This may be the explanation for the slight (although not statistically significant) improvement noted here in readers' performance on 40:1 compressed images compared with original images.

In conclusion, we studied the effects of a wavelet-based compression scheme on the diagnosis of subtle findings (solitary pulmonary nodules and fibrosis) on 60

TABLE 3
P Values for the Observed Difference between AUC Index of Two ROC Curves (Uncompressed vs 40:1, Uncompressed vs 80:1, and Compressed 40:1 vs 80:1)

Comparison	AUC Uncompressed	AUC Compressed 40:1	AUC Compressed 80:1	P Value (uncompressed vs 40:1)	P Value (uncompressed vs 80:1)	P Value (compressed 40:1 vs 80:1)
Fibrosis vs others	0.77 (0.06)	0.81 (0.06)	0.79 (0.06)	0.61	0.79	0.82
Fibrosis vs negative cases	0.83 (0.06)	0.88 (0.06)	0.88 (0.05)	0.59	0.55	0.99
Nodules vs others	0.83 (0.07)	0.86 (0.06)	0.85 (0.06)	0.75	0.85	0.90
Nodules vs negative cases	0.85 (0.07)	0.88 (0.05)	0.87 (0.05)	0.72	0.80	0.91

Note.—Numbers in parentheses are standard deviations.

chest radiographs examined by three board-certified radiologists subspecialized in thoracic imaging. Readings were performed in a double-blind protocol followed by a statistical nonparametric ROC evaluation. This design rigorously tested the compression algorithm and gives a high level of confidence that the conclusions are valid.

We found no statistically significant degradation of diagnostic accuracy between images compressed at 40:1 or 80:1 and original images. Moreover, the compressed images, especially those compressed at 40:1, had a slight (though not statistically significant) tendency to yield more accurate diagnosis than the original images, possibly due to noise removal.

While some authors have evaluated a compression method by grouping several image types together, we believe that each image type requires individual evaluation. This type of study, which assesses diagnostic preservation of a lossy compression scheme, should be performed individually on images obtained with each modality and each potential pathologic condition before considering its integration into an imager or other medical device. As the knowledge and understanding of the effects of our lossy compression scheme have increased over the past 2 years and results have shown a high level of image quality, we are now designing new studies intended to provide a strong validation of other radiographs, ultrasound scans, CT scans, and MR images by using similar ROC analysis.

References

1. Siegel EL, Diaconis JN, Pomerantz S, Allman R, Briscoe B. Making filmless radiology work. J Digit Imaging 1995; 8:151–155.
2. Wong S, Zaremba L, Gooden D, Huang HK. Radiologic image compression: a review. Proc IEEE 1995; 83:194–218.
3. Karson TH, Chandra S, Morehead AJ, Stewart WJ, Nissen SE, Thomas JD. JPEG compression of digital echocardiographic images: impact on image quality. J Am Soc Echocardiogr 1995; 8:306–318.
4. Kuduvalli GR, Ranganyan RM. Performance analysis of reversible image compression techniques for high-resolution digital teleradiology. IEEE Trans Med Imaging 1992; 11:430–445.
5. Cosman PC, Davidson HC, Bergin CJ, et al. Thoracic CT images: effect of lossy image compression on diagnostic accuracy. Radiology 1994; 190:517–524.
6. Cox GG, Cook LT, Insana MF, et al. The effects of lossy compression on the detection of subtle pulmonary nodules. Med Phys 1996; 23:127–132.
7. Erickson BJ, Manduca A, Persons KR, et al. Evaluation of irreversible compression of digitized PA chest radiographs. J Digit Imaging 1997; 10:97–102.
8. Persons KR, Palisson P, Manduca A, Erickson BJ, Savcenko V. An analytical look at the effects of compression on medical images. J Digit Imaging 1997; 10:60–66.
9. Said A, Pearlman W. Image compression using the spatial-orientation tree. In: IEEE international symposium on circuits and systems. Piscataway, NJ: IEEE, 1993; 279–282.
10. Manduca A. Medical image compression with wavelet/subband coding. IEEE Eng Med Biol 1995; 14:639–646.
11. Antonini M, Barlaud M, Mathieu P, Daubechies I. Image coding using wavelet transform. IEEE Trans Image Proc 1992; 1:205–220.
12. Hanley JA, McNeil BJ. A method of comparing the areas under receiver operating characteristic curves derived from the same cases. Radiology 1983; 148:839–843.
13. Metz CE. ROC methodology in radiologic imaging. Invest Radiol 1986; 21:720–733.
14. Metz CE. Some practical issues of experimental design and data analysis in radiological ROC studies. Invest Radiol 1989; 24:234–245.
15. Jiang Y, Metz CE, Nishikawa RM. A receiver operating characteristic partial area index for highly sensitive diagnostic tests. Radiology 1996; 201:745–750.
16. Swets JA, Pickett RM. Evaluation of diagnostic systems. New York, NY: Academic, 1982; 80–93.
17. Barten P. Evaluation of the effect of noise on subjective image quality. Proc SPIE 1991; 1453:2–15.
18. Nill N, Bouzas B. Objective image quality measure derived from digital image power spectra. Opt Eng 1992; 31:813–825.
19. Good W, Lattner S, Maitz G. Evaluation of image compression using plausible "non visually weighted" image fidelity measures. Proc SPIE 1996; 2707:301–309.
20. Lattner S, Good W, Maitz G. Visually weighted assessment of image degradation resulting from image compression. Proc SPIE 1996; 2707:507–518.
21. Center for Devices and Radiological Health of the Food and Drug Agency. Guidance for the content and review of 510(k) notifications for picture archiving and communication systems and related products. Federal Register, December 12, 1993.
22. MacMahon H, Doi K, Sanada S, et al. Data compression: effect on diagnostic accuracy in digital chest radiography. Radiology 1991; 178:175–179.
23. Sayre J, Aberle DR, Boechat I, et al. Effect of data compression on diagnostic accuracy in digital hand and chest radiography. Proc SPIE 1992; 1653:232–240.
24. Ishigaki T, Sakuma S, Ikeda M, Itoh Y, Suzuki M, Iwai S. Clinical evaluation of irreversible image compression: analysis of chest imaging with computed radiography. Radiology 1990; 175:739–743.
25. Goldberg MA, Pivovarov M, Mayo-Smith WW, et al. Application of wavelet compression to digitized radiographs. AJR 1994; 163:463–468.
26. Stitik FP, Pockman MS. Radiographic screening in the early detection of lung cancer. Radiol Clin North Am 1978; 16:347–366.
27. Cosman PC, Gray RM, Olshen RA. Evaluating quality of compressed medical images: SNR, subjective rating, and diagnostic accuracy. Proc IEEE 1994; 82:919–932.
28. Harrington MB. Some methodological questions concerning receiver operating characteristic (ROC) analysis for assessing image quality in radiology. J Digit Imaging 1990; 3:211–218.
29. Donoho DI, Johnstone IM. Ideal denoising in an orthonormal basis chosen from a library of bases. Comptes Rendus Acad Sci 1994; 319:1317–1322.